Antigenic Peptide Binding to the Mouse Major Histocompatibility Complex Class II Protein I-E^k. Peptide Stabilization of the Quarternary Structure of I-E^k

Stephan N. Witt and Harden M. McConnell*

Contribution from the Department of Chemistry, Gilbert Laboratory of Biological Sciences, Stanford University, Stanford, California 94305. *Received September 27, 1991*

Abstract: Major histocompatibility complex (MHC) class II MHC proteins are noncovalently associated heterodimeric ($\alpha\beta$) molecules that bind and display antigenic peptides to CD4$^+$ T cells. In the present work, three reactions were investigated: (i) the binding of a fluoresceinated peptide (representing residues 89-104 of pigeon cytochrome *c*, FpCyt*c*) to the purified mouse MHC class II protein I-E^k; (ii) heterodimer disassembly ($\alpha\beta \rightarrow \alpha + \beta$); and (iii) the dissociation of FpCyt*c* from preformed complexes (I-E^k-FpCyt*c*). At pH 5.2, in the detergent octyl β-D-glucoside, the cleavage of heterodimeric molecules into the individual α and β subunits is inhibited by excess FpCyt*c* but not by the nonbinding peptide representing residues 323-339 of chicken ovalbumin (Ova). The kinetic results are consistent with a reaction mechanism whereby a first-order reaction generates a reactive intermediate which then undergoes competing first- and second-order reactions. The parallel cleavage and binding reactions have the same rate when [FpCyt*c*] $\sim$ 30 μM. The results demonstrate that a class II-peptide complex is significantly less prone to cleavage than the reactive heterodimeric intermediate; thus, peptide stabilizes the quarternary structure of MHC class II molecules.

Introduction

The major histocompatibility complex (MHC) is a set of genes found in all vertebrates that encode for three classes of immune-related cell-surface macromolecules.[1,2] MHC class II molecules are found on specialized cells of the immune system such as macrophages, dendritic cells, and B-cells; these cells proteolytically degrade foreign proteins into peptides,[3] which then bind to the class II molecules.[4] The resultant class II-peptide complexes are displayed on the cell-surface and engage in cell-cell communication with helper T-cells (CD4$^+$).[5] Each organism possesses a limited number of different MHC class II molecules. The MHC molecules have evidently evolved to have a dual responsibility with respect to peptide binding. Each MHC molecule can bind many different peptides and retains each of these peptides in its binding site for long periods of time, of orders of hours or days. Thus, the common paradigm of the association of high specificity and high affinity (and low off-rates) is not applicable to these complexes. Unique structural and kinetic mechanisms may be required to understand these unusual complexes.

MHC class II proteins are composed of noncovalently associated α ($\sim$32 kD) and β ($\sim$28 kD) subunits. Each subunit is a transmembrane glycoprotein with four domains. The extracellular domain of the intact heterodimer contains the polymorphic region and is thought to contain the binding site for antigens. No X-ray crystallographic data are available for any MHC class II protein. A model for the structure of class II proteins has been proposed based on the crystal structure of the homologous MHC class I molecule, HLA-A2.[6] For a review of MHC class II protein structure and function see ref 7.

Previous equilibrium binding and kinetic studies have uncovered two significant features relating to MHC class II-peptide interactions. Only a fraction (10-60%) of the binding sites of affinity purified molecules become occupied with added peptide after long incubation periods.[8,9] Both complex formation and peptide dissociation from preformed complexes is very slow ($t_{1/2} \sim$ 10-100 h).[9,10] The low binding can be attributed to the occupation of most binding sites with endogenous peptides.[11] It has been assumed that a small fraction of the class II molecules with unoccupied binding sites participates in the reaction with added peptide. Thus second-order rate constants for peptide binding have been obtained by dividing a pseudo first-order rate constant by the concentration of peptide used in the experiment.[9,12,13] Recent work has shown that the reaction between peptide and mouse MHC class II molecules is nearly zero-order in the peptide concentration for a wide range of peptide concentrations.[14,15] Thus the reported binding rate constants are not valid. A peptide-protein binding reaction that is nearly zero-order in peptide concentration is consistent with an obligatory first-order reaction that precedes the binding step. The first-order reaction may involve a conformational change and/or the release of endogenous peptides that occupy the binding sites of class II molecules. To date, there has been no determination of the second-order rate constant for antigenic peptides binding to MHC class II molecules.

Here we report that the obligate first-order reaction and heterodimer cleavage are both promoted by the detergent octyl glucoside at pH 5.2. An important result to emerge from this study is that the cleavage of heterodimeric I-E^k molecules to α and β subunits is inhibited in a peptide-specific manner. Simulations show that rapid binding and rapid cleavage reactions are consistent with long half-times for complex formation.

Experimental Section

Reagents. Unless otherwise indicated, all chemicals were purchased from Sigma. Fluorescent peptides were labeled at the N-terminus with the succinimidyl ester of 5-(and-6)carboxyfluorescein as described (pCyt*c*89-104: AERADLIAYLKQATAK; Ova323-339: ISQAVHAAHAEINEAGR).[15] I-E^k was obtained from CH27 cells[16] and purified using a 14.4.4S monoclonal antibody[17] affinity column as described.[15]

*To whom correspondence should be addressed.

(1) Schwartz, R. H. *Annu. Rev. Immunol.* **1985**, *3*, 237-261.
(2) Townsend, A.; Bodmer, H. *Annu. Rev. Immunol.* **1989**, *7*, 601-624.
(3) Grey, H. M.; Chesnut, R. *Immunol. Today* **1985**, *6*, 101-106.
(4) Rothbard, J. B.; Gefter, M. L. *Annu. Rev. Immunol.* **1991**, *9*, 527-565.
(5) Livingstone, A. L.; Fathman, C. G. *Annu. Rev. Immunol.* **1987**, *5*, 477-540.
(6) Brown, J. H.; Jardetzky, T.; Saper, M. A.; Samraoui, B.; Bjorkman, P. J.; Wiley, D. C. *Nature* **1988**, *332*, 845-850.
(7) Kaufman, J. F.; Auffray, C.; Korman, A. J.; Shackelford, D. A.; Strominger, J. *Cell* **1984**, *36*, 1-13.
(8) Babbit, B.; Allen, P. M.; Matsueda, G.; Haber, E.; Unanue, E. R. *Nature* **1985**, *317*, 359-361.
(9) Buus, S.; Sette, A.; Colon, S. M.; Jenis, D. M.; Grey, H. M. *Cell* **1986**, *47*, 1071-1077.
(10) Sadegh-Nasseri, S.; McConnell, H. M. *Nature* **1989**, *337*, 274-276.
(11) Buus, S.; Sette, A.; Colon, S. M.; Grey, H. M. *Science* **1988**, *242*, 1045-1047.
(12) Roche, P. A.; Cresswell, P. *J. Immunol.* **1990**, *144*, 1849-1856.
(13) Roof, R. W.; Luescher, I. F.; Unanue, E. R. *Proc. Natl. Acad. Sci. U.S.A.* **1990**, *87*, 1735-1739.
(14) Tampé, R.; McConnell, H. M. *Proc. Natl. Acad. Sci. U.S.A.* **1991**, *88*, 4661-4665.
(15) Witt, S. N.; McConnell, H. M. *Proc. Natl. Acad. Sci. U.S.A.* **1991**, *88*, 8164-8168.
(16) Haughton, G.; Arnold, L. W.; Bishop, G. A.; Mercolino, T. J. *Immunol. Rev.* **1986**, *93*, 35-51.

0002-7863/92/1514-3506$03.00/0

The only modification of the purification procedure is that after extensive washes of the affinity column with a 10 mM phosphate/150 mM NaCl buffer containing 1% (w/v) octyl β-D-glucoside (OG) at pH 7.4, I-E^k was eluted with a solution of 0.1 M Na_2CO_3, 0.5 M NaCl, and 1% (w/v) OG at pH = 11.3. Fractions were immediately neutralized by the addition of an aliquot of 2 M Tris/1% (w/v) OG at pH = 7.0. Fractions containing protein were pooled and dialyzed for 24 h against the sample buffer (10 mM phosphate/150 mM NaCl/0.02% (w/v) NaN_3/1% (w/v) OG at pH = 7.0). All steps took place at 4 °C. Protein concentration was determined by the method of Lowry. The protein was stored at 4 °C until ready for use.

Sample Preparation. After the addition of an aliquot of concentrated peptide to a sample of I-E^k, complex formation was initiated by a simultaneous pH and temperature jump. The sample pH was rapidly adjusted from pH 7.0 to 5.2 by the addition of concentrated citrate buffer (1 M citrate/150 mM NaCl at pH 4.8). The final citrate concentration was 100 mM. The sample was immediately placed in a 37 °C incubator. Aliquots (50–100 μL) were periodically removed and injected on the HPSEC to determine the extent of reaction. Upon injection, a sample underwent a second pH jump since the column was maintained in a phosphate buffer at pH = 7.0.

Complexes of I-E^k–FpCyt*c* were obtained during the course of experiments in which I-E^k was incubated with excess pigeon cytochrome *c* peptide by collecting the fraction at 14–16 mL (Figure 1a,c,e). The fraction was stored at 4 °C prior to use. Before initiating an experiment, the detergent used in the column buffer (*n*-dodecyl β-D-maltoside) was replaced with the sample detergent (*n*-octyl β-D-glucoside) by the following procedure. The volume of the column fraction was reduced by a factor of ten using a microconcentrator (Centricon no. 30, Amicon). The concentrated sample was injected in 200-μL aliquots on to the HPSEC column equilibrated in the sample buffer (10 mM phosphate/150 mM NaCl/0.02% (w/v) NaN_3/1% (w/v) OG, pH = 7.0), and the fraction containing complex (14–16 mL) was once again collected and concentrated. (The column was not maintained in the sample buffer due to the prohibitive expense of octyl glucoside.) To initiate the peptide dissociation experiments, the concentrated sample of preformed complexes was placed in an ice bath, and citrate buffer was added to adjust the pH to 5.2. The cold sample was immediately injected on the TSK G3000SW column to establish an initial value for the amount of complex; the sample was placed in a 37 °C incubator.

Gel Electrophoresis. SDS/PAGE was conducted using a 6% and 12.5% (wt/vol) acrylamide upper and lower gel,[18] at pH 6.5 and 8.6, respectively. Prior to loading onto the gel, all samples were neutralized with 2 M TRIS. The samples were not boiled or reduced with mercaptoethanol before loading onto the gel. Protein was visualized by silver staining.[19]

Gel Filtration Chromatography. A Pharmacia TSK G3000SW high performance gel filtration column (7.5 × 600 mm) with a TSK SWP precolumn (7.5 × 75 mm) was used in the experiments described here. The column eluant was directed through a Gilson Model 121 fluorometer and a standard HPLC absorbance detector setup in series. A 490-nm excitation filter and a 520-650-nm emission filter were used to detect the I-E^k–FpCyt*c* complexes, while protein absorbance was monitored at 275 nm. HPSEC experiments were conducted using a column buffer consisting of 10 mM phosphate, 150 mM NaCl, 0.02% (w/v) azide, and 1 mM *n*-dodecyl β-D-maltoside, at pH = 7.0. Standard solutions of 5-carboxyfluorescein were used to estimate the amount of FpCyt*c*(89–104) bound to I-E^k. Porcine thyroglobulin (600 kD) was used to determine the column void volume (V_0 = 10.4 mL). The flow-rate was 1 mL/min.

Results

The facile separation of high molecular weight protein–peptide complexes (~65 kD) from free peptide (~2 kD) by high performance size exclusion chromatography (HPSEC) was exploited in this study. The reactions to be described are quite slow, with half-times of hours, thus negligible reaction occurs during transit on the column (15 min). Appreciable complex formation has been reported between pH 4.5–5.5.[15,20,21] All reactions were conducted at pH = 5.2.

Complex Formation Kinetics Were Investigated by Incubating I-E^k with Excess FpCyt*c* and Periodically Injecting Aliquots at the Indicated Times To Assess the Amount of Complex Formation. The fluorescence- and absorbance-detected chromatograms shown in Figure 1 were obtained over the course of a 143-h incubation of a sample of I-E^k with excess FpCyt*c* (434 μM). The chromatograms are characterized by a very weak band at 10 mL, a band at 14.6 mL, and a broad band at V_e > 18 mL from excess free peptide. Our previous work has established that the band at 14.6 mL is due to heterodimeric I-E^k molecules. We refer to the band at 14.6 mL in the fluorescence-detected chromatograms as the αβ-FpCyt*c* signal and the same band in the absorbance-detected chromatograms as the heterodimer signal.

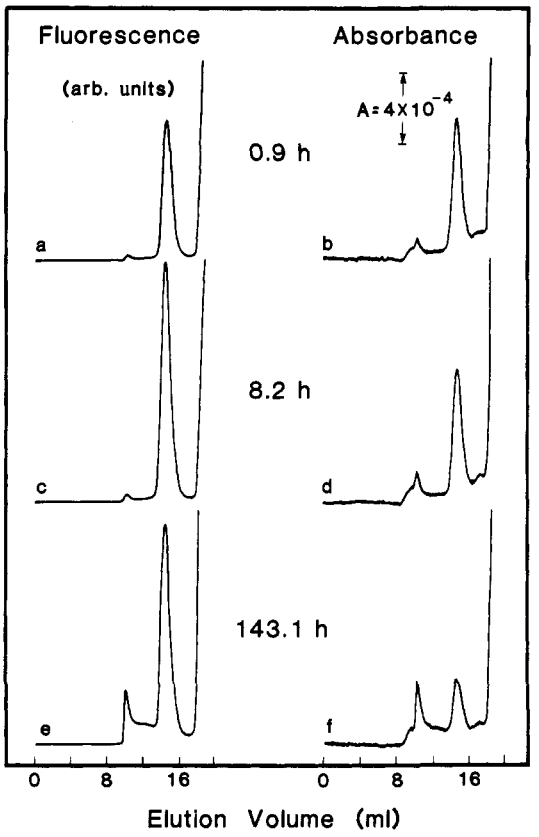

Figure 1. I-E^k–FpCyt*c* complex formation monitored via fluorescence and absorbance-detected high performance size exclusion chromatography. Chromatograms were obtained over the course of a 143-h incubation: traces a and b, 0.9 h; traces c and d, 8.2 h; and traces e and f, 143.1 h. Fluorescence-detected chromatograms: traces a and e, fluorescence sensitivity = 0.05; trace c, fluorescence sensitivity = 0.2. Absorbance-detected chromatograms: traces b, d, and f, full-scale absorbance = 0.002. Sample temperature = 37 °C. Injection volume = 50 μL. Sample pH = 5.2. [I-E^k] = 0.5 μM; [FpCyt*c*] = 434 μM.

In the fluorescence-detected chromatograms, the αβ-FpCyt*c* signal increases through the first 30 h of incubation (a, c) and then slowly loses intensity (e). The companion absorbance-detected chromatograms also show the disappearance of the heterodimer signal during the incubation (b, d, f). The loss of heterodimer signal results from the formation of separate α and β subunits.[18] Related experiments have shown that α and β subunits elute together at 18.1 mL (data not shown) and are thus obscured by the broad signal from excess FpCyt*c* and by detergent micelles (V_e ~ 18-19 mL).[15] The band at 10 mL, which gains intensity after long incubation times (*t* > 4 days), probably arises from aggregation of the liberated α and β subunits (e, f). Complex formation, heterodimer cleavage, and FpCyt*c* dissociation from preformed complexes were investigated by monitoring the peak height of the signal at 14.6 mL.

The complex formation curves show an initial growth in the αβ-FpCyt*c* signal that is abolished at long times (Figure 2A). Complex formation curves at early times are characterized by the following features. (i) After a 31.5-h incubation period with 434 μM FpCyt*c* only 11% of the binding sites are occupied with

(17) Ozato, T.; Mayer, N.; Sachs, D. *J. Immunol.* **1980**, *124*, 533–540.
(18) Dornmair, K.; Rothenhausler, B.; McConnell, H. M. *Cold Spring Harbor Symp. Quant. Biol.* **1989**, *54*, 409–416.
(19) Heukeshoven, J.; Dernick, R. *Electrophoresis* **1985**, *6*, 103–112.
(20) Jensen, P. E. *J. Exp. Med.* **1990**, *171*, 1779–1784.
(21) Harding, C. V.; Roof, R. W.; Allen, P. M.; Unanue, E. R. *Proc. Natl. Acad. Sci. U.S.A.* **1991**, *88*, 7170–7174.

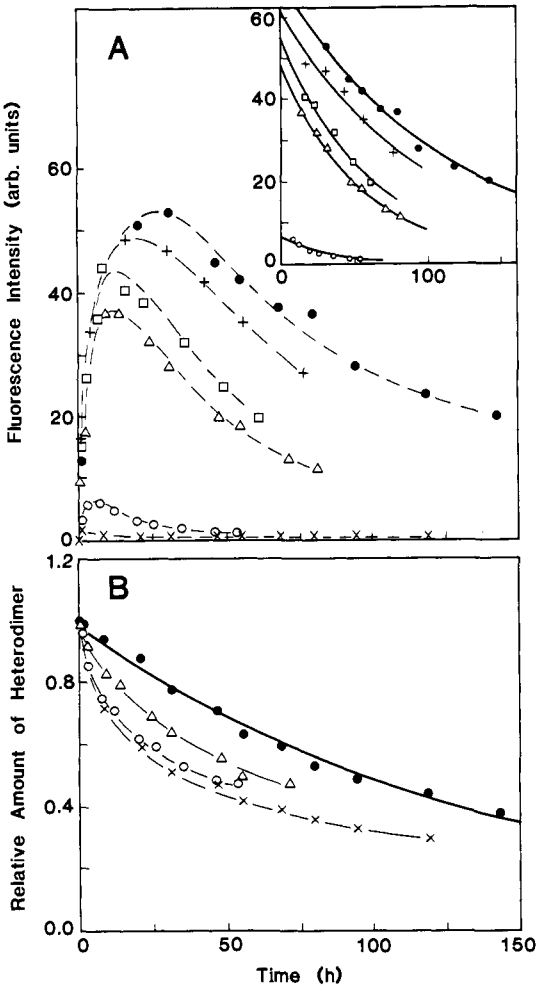

Figure 2. I-E^k–FpCyt*c* complex formation and heterodimer cleavage kinetics. Samples were incubated with excess FpCyt*c* at pH 5.2. Fluorescence- and absorbance-detected chromatograms were obtained for each injection to assess the amount of complex formation and to monitor the change in the total population of heterodimeric molecules. Panel A (fluorescence): ●, 434 μM FpCyt*c*; +, 280 μM FpCyt*c*; □, 140 μM FpCyt*c*; △, 75 μM FpCyt*c*; ○, 5 μM FpCyt*c*; and ×, 500 μM F-Ova. (A, inset) The descending portion of each formation curve was fit to an exponential function (solid lines). Panel B (absorbance): ●, 434 μM FpCyt*c*; △, 75 μM FpCyt*c*; ○, 5 μM FpCyt*c*; and ×, 500 μM F-Ova. The data points obtained at 434 μM FpCyt*c* were fit line to a single exponential (solid line). Conditions: sample pH = 5.2; sample temperature = 37 °C. The data sets in A were normalized to the same gain, injection volume, and protein concentration (170 nM). The data sets in B were normalized by dividing the heterodimer signal $H(t)$ by the signal at t = 0 (H_0), obtained by extrapolating the kinetic curve to zero time. The dashed lines through the data points are to help guide the eye.

FpCyt*c* ([FpCyt*c*]/[I-E^k]$_0$ = 11%). (ii) The maxima of the formation curves shift to longer times as the peptide concentration is increased. At 5 and 434 μM FpCyt*c*, for example, the maximal signal intensity occurs at 5 and 30 h, respectively. (iii) Irrespective of the concentration of FpCyt*c*, the time required to reach one-half of the maximum signal is ~5 h. A sample of I-E^k was incubated with a large excess of the nonbinding peptide FOva as a negative control. (Ova binds to I-A^d but not I-E^{k22}.) The insignificant amount of I-E^k-FOva complex formation shows that there is negligible nonspecific binding.

The gradual loss of $\alpha\beta$-FpCyt*c* signal in the presence of excess FpCyt*c* indicates that the absolute number of complexes *decreases* during the prolonged incubations at pH = 5.2 (Figure 2A). We assume that the reduction is due to a heterodimer cleavage reaction: $\alpha\beta$-FpCyt*c* complexes either split to form subunit–peptide complexes (eq 1), or peptide dissociates and then empty heterodimers split and form subunits that are devoid of bound peptide (eqs 2 and 3). The two splitting reactions may be distinguished.

$$\alpha\beta\text{-Fp} \rightarrow \alpha + \beta\text{-Fp or } \alpha\text{-Fp} + \beta \quad (1)$$

$$\alpha\beta\text{-Fp} \rightarrow \alpha\beta + \text{Fp} \quad (2)$$

$$\alpha\beta \rightarrow \alpha + \beta \quad (3)$$

For the present, the cleavage of $\alpha\beta$-FpCyt*c* complexes is assumed to be independent of the peptide concentration. In contrast, the cleavage of heterodimers by reaction 3 is inhibited by increased peptide since the concentration of $\alpha\beta$ is reduced by the back reaction 4. In other words, if increasing peptide concentration inhibits splitting, we conclude that the splitting proceeds by reaction 3.

$$\alpha\beta + \text{Fp} \rightarrow \alpha\beta\text{-Fp} \quad (4)$$

To determine the half-time for the loss of $\alpha\beta$-FpCyt*c* signal, the decending portion of each kinetic curve was fit to an exponential function (Figure 2A, inset). A variation of the peptide concentration from 5 to 434 μM produces a 3.5-fold *increase* in the half-time to 77 h (Table I). The observed concentration dependence of $t_{1/2}$ for the loss of $\alpha\beta$-FpCyt*c* signal is consistent with the reactions depicted in eqs 2–4.

During the course of obtaining the complex formation data the very weak heterodimer absorbance signal at 14.6 mL was simultaneously monitored. The loss of heterodimer signal occurs with first-order kinetics ($t_{1/2}$ = 96 h; $k_{obs} = 2.0 \times 10^{-6}$ s^{-1}) in the limit of a very large excess of FpCyt*c* (434 μM) (Figure 2B). In contrast, when I-E^k is incubated with a comparably large excess of FOva, 30% of the heterodimer signal is lost within a relatively short time (8 h), while the remaining reduction occurs over a much longer time span (100 h). The biphasic loss of heterodimer signal $H(t)$ follows eq 5,

$$H(t)/H_0 = 0.39 \exp(-k_f t) + 0.61 \exp(-k_s t) \quad (5)$$

where $k_f = 2.8 \pm 0.6 \times 10^{-5}$ s^{-1} and $k_s = 1.6 \pm 0.3 \times 10^{-6}$ s^{-1}, respectively. Nearly identical biphasic curves are obtained when samples are incubated without any added peptide (data not shown) and with a low concentration of FpCyt*c* (5 μM). At an intermediate concentration of FpCyt*c* (75 μM), the kinetic curve falls between the two curves obtained under the extreme conditions of excess binding peptide and nonbinding peptide. On the basis of the fits of the kinetic curves, approximately 40% of the heterodimeric molecules in a sample of affinity purified I-E^k are active and susceptible to cleavage. The remaining molecules are unreactive to FpCyt*c*, presumably due to peptides of unknown composition occupying the binding sites.

SDS/PAGE Was Employed To Verify that Subunit Formation Is Inhibited by Excess pCyt*c*. SDS/PAGE separates heterodimeric molecules from individual subunits, and since low molecular weight species are not retained by the gel, α and β subunits are readily detected. Identically prepared samples of I-E^k were incubated with either a large excess of pCyt*c* (1.65 mM) or Ova (1.7 mM) at pH = 5.2. Aliquots were removed at 24 and 96 h

Table I. Experimental and Calculated Half-Times versus Peptide Concentration for the Loss of I-E^k–FpCyt*c* Signal in the Decay Portion of the Formation Curves[a]

		simulation	
[FpCyt*c*] (μM)	exptl $t_{1/2}$ (h)	k_2 = 1 M^{-1} s^{-1} $t_{1/2}$ (h)	k_2 = 1000 M^{-1} s^{-1} $t_{1/2}$ (h)
5	22 ± 3	10	7
75	36 ± 2	25	19
139	48 ± 6	38	32
280	57	64	58
434	77	96	88

[a] Experimentally observed half-times (mean ± s.e.m.) for the loss of the $\alpha\beta$-FpCyt*c* signal were obtained by fitting the decay to an exponential function (Figure 2A, inset). Simulated curves were analyzed in the same way.

(22) Buus, S.; Sette, A.; Colon, S. M.; Miles, C.; Grey, H. M. *Science* **1987**, *235*, 1353–1358.

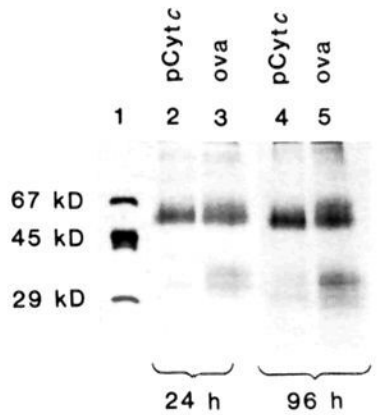

Figure 3. Inhibition of the heterodimer cleavage reaction visualized by SDS/PAGE. One sample of I-E^k was incubated with 1.65 mM pCyt*c*; an identically prepared sample was incubated with 1.7 mM Ova. Aliquots were removed after 24 and 96 h of incubation and were assayed with SDS/PAGE: lane 1, standards, bovine serum albumin (67 kD), chicken albumin (45 kD), and carbonic anhydrase (29 kD); lane 2, 24-h incubation with pCyt*c*; lane 3, 24-h incubation with Ova; lane 4, 96-h incubation with pCyt*c*; and lane 5, 96-h incubation with Ova. Sample pH = 5.2. Prior to loading, samples were neutralized with an aliquot of concentrated TRIS buffer. [I-E^k] = 0.9 μM; 45 μL of sample were loaded per well.

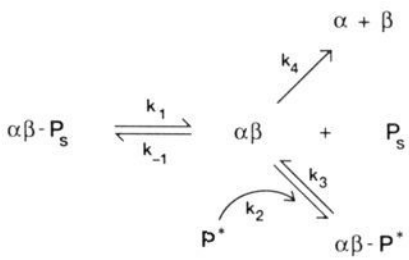

Figure 4. Proposed mechanism for MHC class II–peptide complex formation.

and assayed for subunit formation by SDS/PAGE without prior boiling or reduction of the samples. The results are shown in Figure 3.

After a 24-h incubation period, the protein remains in the heterodimeric state for the sample of I-E^k incubated with excess pCyt*c* (lane 2). In contrast, after the same incubation period, α and β subunits are detected in the sample of I-E^k incubated with an excess Ova (1.7 mM) (lane 3). Focussing on lane 3, most of the molecules are in the heterodimeric state, although a small portion has cleaved to form the α and β subunits. Upon continued incubation (96 h), the amount of free chains appears to increase in the sample incubated with the nonbinding peptide (lane 5) compared to the sample incubated with pCyt*c* (lane 4). The SDS/PAGE experiments are consistent with the results shown in Figure 2A,B. The results from the HPSEC and SDS/PAGE experiments are consistent with the reaction mechanism depicted in Figure 4, discussed later.

The Kinetics of Peptide Dissociation from Preformed Complexes of I-E^k–FpCyt*c* Were Investigated by Incubating Complexes in Octyl Glucoside at pH = 5.2 for Approximately 24 h. The chromatograms shown in Figure 5 were obtained over the course of a 24-h incubation of preformed I-E^k–FpCyt*c* complexes at pH = 5.2 without any added peptide. The disappearance of $\alpha\beta$-FpCyt*c* signal can result from either reactions 1 or 2 or both (eqs 1 and 2). The first chromatogram (t = 0) has an intense $\alpha\beta$-FpCyt*c* signal and a very weak feature at V_e = 25 mL from a small amount of FpCyt*c*. Upon continued incubation (t = 7.4 and 12.1 h traces), the $\alpha\beta$-FpCyt*c* signal loses intensity and the free peptide signal gains intensity. Significantly, no signal from either α-FpCyt*c* or β-FpCyt*c* is observed at the expected position ($V_e(\alpha,\beta)$ = 18 mL); therefore, the splitting reaction shown in eq 1 does not contribute to the reduction in the $\alpha\beta$-FpCyt*c* signal. The

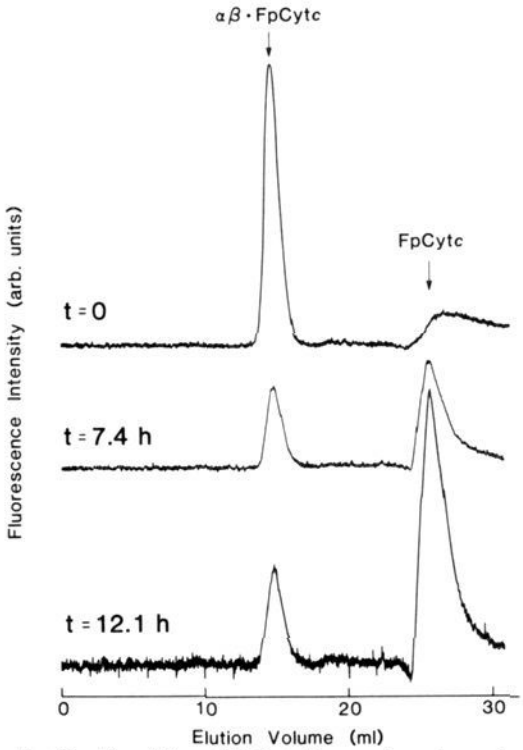

Figure 5. The dissociation of FpCyt*c* from preformed complexes of I-E^k–FpCyt*c* monitored with fluorescence-detected HPSEC. A sample of I-E^k–FpCyt*c* was incubated at pH = 5.2 for 24 h. Aliquots were removed and injected at the indicated times to determine the extent of reaction. In a separate experiment, a dilute sample of FpCyt*c* was injected to determine an accurate elution volume (V_e(FpCyt*c*) = 25.4 mL). Conditions: sample temperature, 37 °C; amount injected, 200 μL; fluorescence sensitivity, 0.01 (t = 0.0 and 7.4 h traces); fluorescence sensitivity = 0.005 (t = 12.1 h trace).

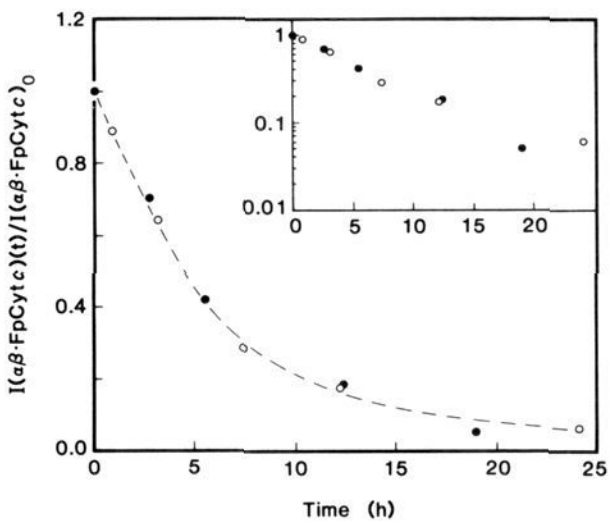

Figure 6. The dissociation of FpCyt*c* from preformed complexes of I-E^k–FpCyt*c* at pH 5.2. Preformed complexes were incubated with either no added peptide (○) or with 150 μM unlabeled pCyt*c* (●). The half-time for the loss of I-E^k–FpCyt*c* signal shows no dependence on pCyt*c* ($t_{1/2}$ = 5.2 h; $k_3 = 3.7 \pm 0.4 \times 10^{-5}$ s^{-1}). For each curve, the peak height of the first time point, I($\alpha\beta$-FpCyt*c*)$_0$, was used to normalize the data. The dashed line through the data is to help guide the eye. (Inset) A semilog plot of the data points.

results are consistent with the loss of $\alpha\beta$-FpCyt*c* signal due to peptide dissociation from preformed complexes to form two products, empty heterodimer and FpCyt*c*.

The $\alpha\beta$-FpCyt*c* signal intensity versus time profiles are shown in Figure 6. The dissociation of FpCyt*c* follows first-order kinetics

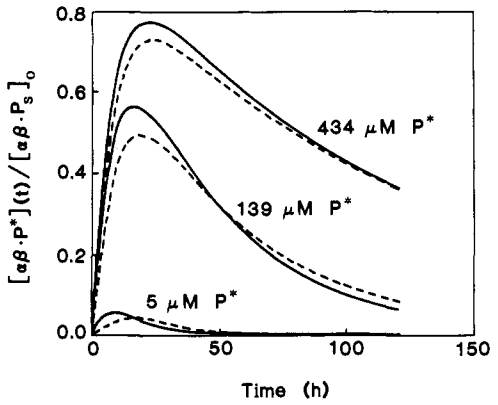

Figure 7. Simulated complex formation curves with $k_4/k_2 = 30$ μM. Curves were obtained with $k_2 = 1$ M^{-1} s^{-1} and $k_4 = 3 \times 10^{-5}$ s^{-1} at 5, 139, and 434 μM added peptide (dashed lines). At the same concentrations of added peptide, simulations with $k_2 = 1000$ M^{-1} s^{-1} and $k_4 = 3 \times 10^{-2}$ s^{-1} yield the solid curves. Simulations were conducted by numerically integrating the rate equations associated with the proposed reaction mechanism (Figure 4). The following assumptions were made: $k_{-1} = k_2$ and $k_1 = k_3 = 3.7 \times 10^{-5}$ s^{-1}.

(inset). The peptide dissociation experiments were conducted with and without a large excess of unlabeled pigeon cytochrome *c* peptide. Excess unlabeled pCyt*c* does not affect the half-time for the dissociation of bound FpCyt*c* ($t_{1/2} = 5.2$ h, $k_3 = 3.7 \pm 0.4 \times 10^{-5}$ s^{-1}). The half-time for the release of FpCyt*c* from preformed complexes is close to the half-time for the formation of complexes (Figure 2A).[15]

Complex Formation Was Simulated Numerically To Test the Proposed Kinetic Mechanism. The above value for the dissociation of FpCyt*c* of $k_3 = 3.7 \times 10^{-5}$ s^{-1} is used. Since fluorescent–peptide complex formation occurs with nearly the same half-time as FpCyt*c* release, it is reasonable to set k_1 equal to k_3 in the reaction scheme in Figure 4. It is assumed that k_{-1} is equal to k_2. Parameter space was explored to find the ratio cleavage/binding = k_4/k_2 that produces the best fits to the observed complex formation and heterodimer decay curves. The ratio of k_4/k_2 is the peptide concentration at which the rate of peptide binding and heterodimer cleavage are the same. We find that the simulated curves reproduce the experimental formation curves when k_4/k_2 is ~30 μM (Figure 7). When k_4/k_2 is less than 30 μM, the simulated curves tend to stable asymptotic values ($30 < t < 200$ h), especially at high concentrations of peptide. Stable asymptotes at long times indicate that the binding reaction dominates the heterodimer cleavage reaction. Conversely, the simulated formation curves have steeper descending portions than those observed experimentally when $k_4/k_2 > 30$ μM, because, under these conditions, heterodimer cleavage dominates peptide binding.

Using $k_4/k_2 = 30$ μM, simulations were conducted with values of k_2 from 0.1 to 10^3 M^{-1} s^{-1}. Figure 7 shows calculated complex formation curves obtained with $k_2 = 1$ and 1000 M^{-1} s^{-1}. The largest difference between the two sets of formation curves is seen at the low peptide concentration (5 μM). At that concentration, maximal complex formation occurs at 16.7 and 9.2 h for values of the binding rate constant of 1 and 1000 M^{-1} s^{-1}, respectively. The experimentally observed maxima are 5 ± 1 h at 5 μM FpCyt*c*. The half-time for the descending portion of each simulated curve was also determined (Table I). Both sets of calculated half-times come close to replicating the experimental values obtained at high ligand concentration (75–434 μM). At 5 μM peptide, the calculated half-times deviate from the experimental half-times by factors of 2–3. The simulations reveal that quite disparate values of k_2 produce formation curves with acceptable agreement with the observed formation curves as long as k_4/k_2 is equal to 30 μM.

Discussion

The Mechanism of MHC Class II–Peptide Complex Formation. It was found in previous work that when I-E^k is incubated under identical reaction conditions to those described here, except that the nonionic detergent dodecyl β-D-maltoside is used, complex formation curves reach nearly stable asymptotes for incubations up to 60–80 h when excess FpCyt*c* is used ([FpCyt*c*]/[I-E^k] > 10).[15] At long times, a reproducible 10–20% reduction in the αβ-FpCyt*c* signal, and in the heterodimer signal, was detected at an equimolar ratio of peptide to protein. These kinetic results in dodecyl maltoside can also be explained in terms of the reaction scheme in Figure 4. The nearly stable asymptotes observed at high ligand concentrations in dodecyl maltoside solution, and in the simulations at $k_4/k_2 < 30$ μM, might be misinterpreted as indicating that equilibrium is reached. Our current work shows that equilibrium is not reached in this system.

The half-time for the loss of αβ-FpCyt*c* signal in the decay portion of the biphasic formation curves depends on the concentration of FpCyt*c*. The formation of free subunits is inhibited by pCyt*c* but not by a nonbinding peptide (Ova). These observations support the mechanism depicted in Figure 4. The reactive intermediate αβ has a shorter life-time than the MHC class II–peptide complex according to the mechanism in Figure 4. Furthermore, the differential loss of αβ-FpCyt*c* signal found in these experiments and in previous experiments is consistent with a detergent-sensitive destabilization of the reactive precursor to form separate α and β chains. We have recently observed that cleavage of I-A^d heterodimeric molecules at low pH to form free subunits is also subject to inhibition by the peptide Ova(323–339).[23] The mechanism depicted in Figure 4 is thus likely to be generally applicable to MHC class II–peptide interactions.

There is a large uncertainty in the magnitude of the rate constants for peptide binding and heterodimer cleavage estimated from kinetic simulations. The life-time of αβ against splitting is somewhere between 20 s and 6 h.

From the amplitude coefficients in eq 5, it is estimated that 40% of the I-E^k molecules in a preparation are potentially active in the experiments with fluorescent peptide. On the basis of the HPSEC results, 30% of these active I-E^k molecules have binding sites occupied with FpCyt*c* after a 31.5 h incubation with 434 μM FpCyt*c* (Figure 2A). The simulated complex formation curves reveal that after 31.5 h of incubation 80% of the sites are occupied (Figure 7). The remaining fraction of I-E^k molecules are inactive because the sites are evidently occupied with tightly bound endogenous peptides.

The results in Figure 3 show that disruption of heterodimers to form α and β subunits is inhibited by a large excess of pCyt*c* but not by Ova. In previous work, it was found that a 30-min incubation of I-E^k at pH = 5 with 100 μM pCyt*c* did not inhibit the disassembly of heterodimeric molecules.[18] The absence of peptide-dependent inhibition in that work is probably due to the different reaction conditions employed in the two studies. The main consideration is that the present gel experiments utilize a large excess of pCyt*c* (1.65 mM). According to the results shown in Figure 2B, a large excess of FpCyt*c* is necessary to inhibit the loss of the heterodimer signal. At 75 μM FpCyt*c*, some inhibition of the loss of heterodimer signal is observed, relative to the curve obtained at 434 μM FpCyt*c*. However, an amount of FpCyt*c*-(89–104) peptide larger than 100 μM seems to be required to achieve a high degree of inhibition.

There is evidence that antigenic peptide has a role in maintaining the three-dimensional structure of MHC class I molecules.[24-27] (MHC class I molecules bind and display endogenous peptides to cytotoxic T-cells.[2]) Until recently, a similar role for peptide in maintaining the structure of class II molecules has not been reported previously. We have shown that peptide binding stabilizes the heterodimer and thereby inhibits the detergent-sensitive disassembly of class II molecules at low pH. Sadegh-

(23) Witt, S. N.; McConnell, H. M. Unpublished results, 1991.
(24) Townsend, A.; Öhlén, C.; Bastin, J.; Ljunggren, H.-G.; Foster, L.; Kärre, K. *Nature* **1989**, *340*, 443–448.
(25) Lie, W.-R.; Myers, N. B.; Gorka, J.; Rubocki, R. J.; Connolly, J. M.; Hansen, T. H. *Nature* **1990**, *344*, 439–441.
(26) Schumacher, T. N. M.; Heemels, M.-T.; Neefjes, J. J.; Kast, W. M.; Melief, C. J. M.; Ploegh, H. L. *Cell* **1990**, *62*, 563–567.
(27) Townsend, A.; Elliot, T.; Cerundolo, V.; Foster, L.; Barber, B.; Tse, A. *Cell* **1990**, *62*, 285–295.

Nasseri and Germain have come to the same conclusion.[28] The mechanism by which a bound peptide exerts control over the conformational state of a class II molecule is unknown. There are several instances of ligand binding either altering or stabilizing the three-dimensional structure of a protein.[29,30]

Acknowledgment. This work was supported by a Damon Runyon-Walter Winchell Cancer Fund Fellowship, DRG-968 (S. N.W.), and by a National Institutes of Health Grant 5R01 AI 13587-13.

Registry No. Cytochrome *c*, 9007-43-6.

(28) Sadegh-Nasseri, S.; Germain, R. N. *Nature* **1991**, *353*, 167–170.
(29) Duportail, G.; Lefevre, J.-F.; Lestienne, P.; Dimicoli, J.-L.; Bieth, J. G. *Biochemistry* **1980**, *19*, 1377–1382.
(30) Khananshvili, D.; Gromet-Elhanan, Z. *Biochemistry* **1986**, *25*, 6139–6144.

Conformation-Controlled Hydrolysis of Polyribonucleotides by Sequential Basic Polypeptides

Bernard Barbier and André Brack*

Contribution from the Centre de Biophysique Moléculaire—CNRS, 1A Avenue de la Recherche Scientifique, 45071 Orléans Cedex 2, France. *Received March 5, 1991*

Abstract: Polycationic polypeptides containing basic and hydrophobic amino acids strongly accelerate the hydrolysis of oligoribonucleotides. We have examined aspects of the oligonucleotide–polypeptide interaction, as well as the relationship among amino acid composition, polypeptide conformation, and the hydrolytic effect. We conclude that, to be active, the polypeptides must present a regular distribution in space of basic groups (β-sheet or α-helix). A tentative model is given involving an alignment of the polynucleotidic chain between two parallel rows of positive charges. The experimental data for the base-induced hydrolysis are consistent with a mechanism involving two basic amino acid side chains.

Introduction

A number of studies have shown that synthetic peptides or polypeptides can exhibit enzyme-like activity. Peptides and copolypeptides with a weak esterasic activity[1-4] and glycosidic activity[5] have been reported. A strong ribonuclease activity was found for a 70-residue synthetic polypeptide analogue of ribonuclease S-protein[6] and with a 34-residue polypeptide and its dimer.[7] More recently,[8] a noticeable activity has been found with a 99-residue polypeptide of an aspartic protease.

Even very simple peptides can show such activities. For example, Lys-Trp-Lys is able to recognize and to cleave DNA strands at apuric or apurinic sites.[9-11] Other simple copolypeptides are known to exhibit weak esterasic activities[12,13] or glycosidic activity.[14]

In two previous communications[15,16] we have briefly reported that basic polypeptides interact with polyribonucleotides and accelerate their hydrolysis. In these first studies, the hydrolyses were run with mixtures of oligoribonucleotides which did not allow an accurate determination of either the rate or the stoichiometry of the reaction. Therefore, the experiments were repeated with well-defined oligoribonucleotides as substrates. In the present paper we describe a number of factors involved in the reaction and propose a model for the mechanism of hydrolysis.

Materials and Methods

$(Ap)_9A$ and poly(A) were purchased from Pharmacia. Oligo(A)s up to the 25-mer were obtained by alkaline hydrolysis of poly(A) in KOH (0.2 M) at room temperature for 10 h. The ring-opening of 2′–3′ cyclic phosphate end groups was performed in aqueous $HClO_4$ at pH 2 for 2 h. Several nucleotides and oligonucleotides were used to calibrate the HPLC chromatograms: A, A2′p, A3′p, and A > p (Sigma), ApA and $(Ap)_2$ (Waldhof), and $(Ap)_2A$, $(Ap)_3A$, and $(Ap)_5A$ (Pharmacia). $(Ap)_3$ was isolated from a mixture of oligo(A)s obtained by alkaline hydrolysis of poly(A) in KOH (0.2 M) at room temperature for 10 h. The $(Ap)_3$ fraction, isolated by ion exchange chromatography on a "strong retention" preparative PVDI 33 column (Société Française Chromato Colonne) was desalted on a G10 Sephadex column (Pharmacia) and finally lyophilized. Poly(L-lysine) and poly(L-histidine) were obtained from Bachem, and poly(L-arginine) was obtained from Sigma. The sequential polypeptides were synthesized in our laboratory: poly(Leu-Lys) and poly(Glu-Leu),[17] poly(Glu-Ser-Glu),[18] poly(Arg-Leu),[19] poly-(D,L-Leu-D,L-Lys),[20] and poly(Leu-Lys-Lys-Leu).[21] The dipeptide CH_3CO-Leu-Lys-NHC_2H_5 (Ac-Leu-Lys-NHEt) was prepared by liq-

(1) Sheehan, J. C.; Benett, G. B.; Schneider, J. A. *J. Am. Chem. Soc.* **1966**, *88*, 3455.
(2) Petz, D.; Schneider, F. *Z. Naturforsch.* **1976**, *31c*, 675.
(3) Trudelle, Y. *Int. J. Pept. Protein Res.* **1982**, *19*, 528.
(4) Nishi, N.; Morishige, M.; Tsutsumi, A.; Nakajima, B. *Int. J. Biol. Macromol.* **1983**, *5*, 42.
(5) Chakravarty, P. K.; Mathur, K. B.; Dhar, M. M. *Experimentia* **1973**, *29*, 786.
(6) Gutte, B. *J. Biol. Chem.* **1975**, *250*, 889.
(7) Gutte, B.; Daumigen, M.; Wittschieber, E. *Nature* **1979**, *281*, 650.
(8) Veber, D. F.; Nutt, R. F.; Brady, S. F.; Nutt, E. M.; Ciccarone, T. M.; Garsky, V. M.; Waxman, L.; Benett, C. D.; Rodkey, J. A.; Sigal, I.; Darke, P. In *Peptide 1988*; Jung, G., Bayer, E., Eds.; Walter de Gruyter: Berlin–New York, 1989; p 190.
(9) Behmoaras, T.; Toulme, J. J.; Helene, C. *Nature* **1981**, *292*, 858.
(10) Pierre, J.; Laval, J. *J. Biol. Chem.* **1981**, *256*, 10217.
(11) Ducker, N. J.; Hart, D. M. *Biochem. Biophys. Res. Commun.* **1982**, *105*, 1433.
(12) Hatano, M.; Nozawa, T. *Prog. Polym. Sci., Jpn.* **1972**, *4*, 223.
(13) Noguchi, J.; Nishi, N.; Tokura, S.; Murakami, U. *J. Biochem. (Tokyo)* **1977**, *81*, 47.
(14) Mathur, K. B.; Chakravarty, P. K.; Srivastava, S.; Dhar, M. M. *Indian J. Biochem. Biophys.* **1971**, *8*, 90–93.
(15) Barbier, B.; Brack, A. *J. Am. Chem. Soc.* **1988**, *110*, 6880.
(16) Brack, A.; Barbier, B. *Origins Life* **1990**, *20*, 139.
(17) Brack, A.; Caille, A. *Int. J. Pept. Protein Res.* **1978**, *11*, 128.
(18) Chaves, J. G.; Trudelle, Y. *J. Polym. Sci.* **1975**, *52*, 125–135.
(19) Barbier, B.; Caille, A.; Brack, A. *Biopolymers* **1984**, 2299–2310.
(20) Brack, A.; Spach, G. *J. Mol. Evol.* **1979**, *13*, 35.
(21) Barbier, B.; Perello, M.; Brack, A. *Collect. Czech. Chem. Commun.* **1988**, *53*, 2825.

0002-7863/92/1514-3511$03.00/0